An Overview of High Fidelity CFD Engine Modeling

Spinner, Sebastian*
DLR Institute of Aerodynamics and Flow Technology, Braunschweig, Germany

Trost, Marco† and Schnell, Rainer‡
DLR Institute of Propulsion Technology, Köln, Germany

In this work we give an overview over state of the art engine performance modeling with CFD. For both flow solvers predominantly used at DLR we show the available methods to model aircraft engine performance with high fidelity. Within the TAU code, a solver mainly used for outer aerodynamics, full annulus uRANS simulations with a rotating fan may be used to model the engine accurately. In RANS simulations an actuator disk method or a body force model are available to represent the fan stage. In the flow solver TRACE, primarily developed to model internal turbomachinery flow, single passage RANS simulations with mixing-planes or uRANS simulations with time-shifted boundary conditions can be used. Additionally full annulus uRANS simulations may be performed as well.

A test case is run with the aforementioned engine modeling methods allowing for comparison and evaluation of the different models. Integral engine performance metrics and radial distributions are compared to assess the capabilities of different simulation approaches. High fidelity 360° uRANS methods deliver accurate results but are costly in terms of time and resources. The RANS methods presented pose as viable alternatives to model engine performance metrics requiring only a fraction of the resources of an unsteady simulation. Single passage uRANS simulations utilizing time shifted boundary conditions fill the gap between full annulus uRANS and RANS methods by simulating unsteady aerodynamic phenomena with an acceptable demand for computational resources.

Nomenclature

α_{out}	=	OGV Outflow Swirl Angle, [°]
η_{is}	=	Isentropic Efficiency, [-]
Π_t	=	Total Pressure Ratio, [-]
$C_{L,min}$	=	Minimum Lift Coefficient
$C_{L,max}$	=	Maximum Lift Coefficient
$\dot{m}_{red}$	=	Reduced Massflow, [kg/s]
M	=	Mach Number, [-]
r/h	=	Nondimensional Channel Height, [-]

ADP	=	Aerodynamic Design Point
CFD	=	Computational Fluid Dynamics
HPC	=	High Performance Computing
OGV	=	Outlet Guide Vane
RANS	=	Reynolds Averaged Navier Stokes
SID	=	Sideline
UHBR	=	Ultra High Bypass Ratio

I. Introduction

Modern commercial transport aircraft depend on efficient propulsion concepts in order to meet the legal and social framework conditions with regard to environmental compatibility. Propulsion concepts like boundary layer ingestion or ultra high bypass ratio (UHBR) engines require a close integration of the propulsion system to the airframe. As a consequence the airframe and engine designers have to work closely together to maximize the potential efficiency gains from these concepts. This demands for new tools to accurately model engine performance during airframe design and integration under different conditions. These tools are required to reliably model the flow physics for a wide range of conditions allowing for exploration of the design space when it comes to engine integration.

*Research Scientist, Transport Aircraft Branch
†Research Scientist, Fan and Compressor Branch
‡Research Scientist, Fan and Compressor Branch

It is of special importance that the engine modeling method is able to account for the effects of non-uniform inflow and variations in angle of attack. This is self-explanatory for concepts like boundary layer ingestion were the boundary layer profile directly affects the engine but the trend towards UHBR engines enforces this requirement as well. The engine core size can not be reduced easily to increase the bypass ratio because the power density required from the core would significantly drive up thermal and structural stresses beyond what current materials can withstand. Therefore increasing the bypass ratio requires the engine diameter to be increased as well. To counteract the weight penalty introduced by the increased engine size UHBR nacelle designs tend towards shortened inlets and nozzles. A shorter inlet is not as effective to align the flow with the fan axis under off-design conditions requiring the fan to cope with non-uniform inflow conditions.

In a first assessment various engine models are tested for their capabilities of to reproduce mean engine performance metrics under different operating conditions. In this work two flow solvers are considered both originating within DLR. The flow solver TAU is an unstructured vertex-based finite-volume solver mainly used for outer aerodynamics investigations [1]. The second solver applied in this work is the flow solver TRACE, a finite-volume based code developed predominantly for internal and turbomachinery applications [2].

II. Example Test Case

The engine studied in this work and used as an example to explain the different engine modeling methods was designed within the EU Clean Sky 2 project ASPIRE and is representative of a generic modern UHBR turbofan. The nacelle geometry was provided by Airbus and is characterized by a very small length-to-diameter ratio. The fan stage was designed by the DLR Institute of Propulsion Technology for application in a geared turbofan engine [3]. It features 16 rotor blades and 36 OGV blades. The ASPIRE fan is well suited for the evaluation of different engine modeling methodologies for various reasons. It has been designed with state of the art tools and is deemed representative for current and near future turbofan designs due to its high bypass ratio, low fan pressure ratio and shortened nacelle. Multiple studies already used this engine as a test case for turbomachinery CFD forming a solid knowledge base allowing to put results obtained with different methods and solvers into context . The engine was used as a benchmark to test and compare different CFD codes for their capability to model an engine with 360° uRANS simulations [4]. In recent studies it was used to evaluate high fidelity engine modeling approaches [5, 6].

III. Numerics

A. TAU

The DLR TAU Code [1] is an unstructured finite-volume vertex-based CFD solver successfully in use at DLR for almost two decades. Within RANS simulations an actuator disk model or a body force approach may be used to model engine performance as described in chapters IV.B andIV.C. There is also the possibility to model the engine by using a 0D thermodynamic boundary condition based on averaged fanstage performance but due to its limitation to only deliver uniform exhaust distributions it is not considered in this work. An additional option is to perform full annulus uRANS simulations of the engine with a rotating fan as presented in chapter IV.A. All TAU simulations presented in this work share a common CFD setup. The computational domain was divided into several blocks meshed individually and being combined using the code's Chimera method [7] as already presented in [6]. This way it was possible to use the same nacelle and farfield meshes for the different TAU methodologies by only exchanging the fan stage meshes.

All TAU simulations presented in this paper were performed fully turbulent using the Spalart Allmaras one-equation turbulence model [8]. Spatial discretization for the convective fluxes was done using a second order central differencing scheme with scalar dissipation for the uRANS and body force simulation. A second order upwind scheme was used for the actuator disk simulation. Multigrid methods and local time stepping were applied to accelerate convergence. For the unsteady simulations a dual time stepping approach was put to use.

B. TRACE

The DLR TRACE code is a hybrid (structured and unstructured) flow solver in continuous development since the beginning of the 1990's. It is being extensively used likewise by german national industry and academia and has been developed predominantly for internal and turbomachinery applications. All mentioned CFD techniques in this work share the same code basis, are formulated based on finite volumes and take advantage of identical and Roe-type flux formulations with 2nd order MUSCL interpolation to the cell vertices. The solver methodology is implicit with second

order temporal accuracy and the Menter SST k–ω turbulence model being applied predominantly. Blade row coupling for the RANS simulation was realized with classical mixing-planes formulated in a non-reflecting manner as described in chapter IV.D. In addition a chorochronic approach using phase-shifted boundary conditions was applied in a uRANS simulation as presented in chapter IV.E.

IV. Engine Modeling Methods

In the following an overview of the underlying principles and technical background of the different engine modeling methods is given. If available the reader is referred to related publications for further reading.

A. uRANS Full Annulus

In TAU a fan engine can be modeled by taking use of the code's Chimera method[7]. The mesh is split into multiple blocks containing the fan, OGV and further geometry. The fan block will then be rotated by means of mesh rotation while the OGV block remains stationary. These mesh blocks can be integrated into any corresponding outer mesh to model isolated or installed engine performance. The engine power setting is thereby defined by setting the rotation speed of the fan mesh block. An example of an isolated engine configuration for the ASPIRE fan with this setup is given in Fig. 1. In front of the fan a dense area of mesh lines indicates the presence of a Chimera overlapping region.

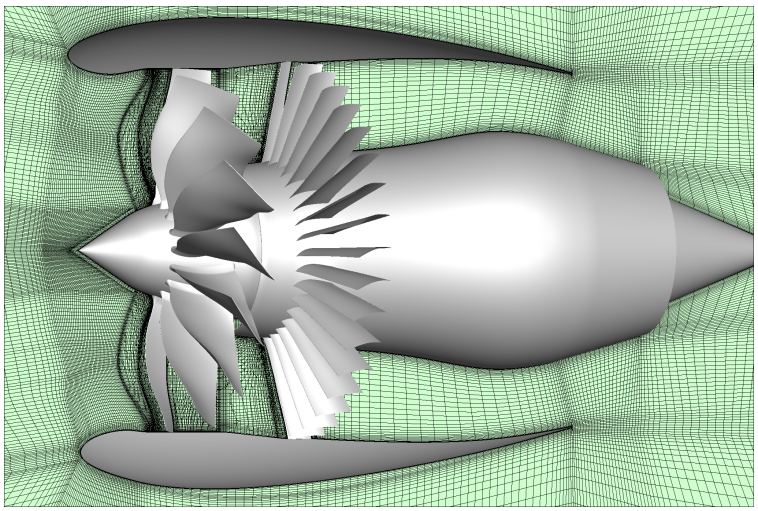

Fig. 1 Visualization of the mesh used for TAU URANS simulations with rotating fan.

The simulations are started with a stationary rotor mesh block to obtain an initial steady solution for the flow around the nacelle. Experience shows that this approach significantly accelerates convergence during the unsteady phase of the simulation. Subsequently the rotor rotation is activated and the solver is switched to unsteady mode. In the beginning of the unsteady phase a large time step is chosen to resolve the rotor rotation which is then further refined step by step up to a time step at which the rotor mesh is only rotated by one cell width compared to the OGV mesh. A detailed description on mesh generation, impact of temporal resolution and mesh convergence as well as a thorough analysis of the aerodynamics can be found in [9].

B. RANS Actuator Disk

The actuator disk model is implemented as a boundary condition into the finite volume method of TAU. When using the actuator disk model the blades are replaced by a disk of zero thickness. This disk imposes a jump in pressure to the flow whereas the velocity remains constant. Additionally flow turning is introduced based on the corresponding forces. When modeling fan engines with the actuator disk model both the rotor and the OGV must each be represented by a separate disk. The actuator disk configuration of the engine investigated in this work is shown in Fig. 2. The mesh contains the same nacelle mesh block with only the region of rotor and OGV remeshed. Note that Chimera and structured meshes are used in this case to ensure consistency with the other methods investigated but this is no prerequisite of the actuator disk model.

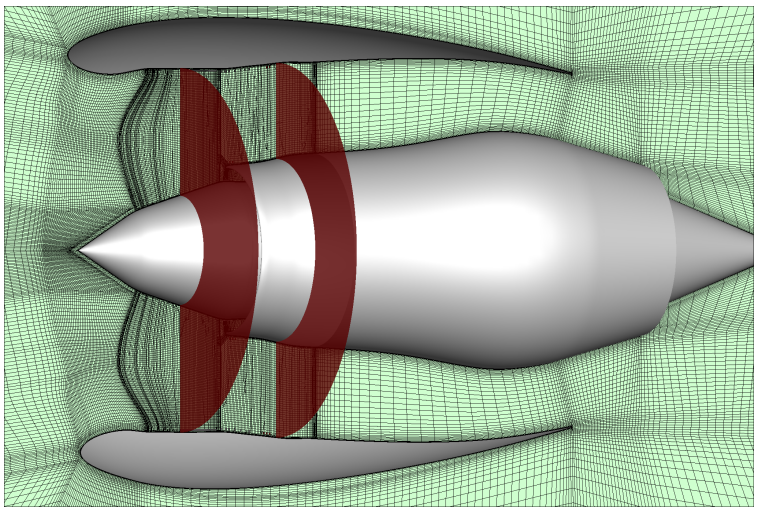

Fig. 2 Visualization of the mesh used for TAU RANS simulations with actuator disk boundary conditions.

To perform actuator disk simulations an individual input data set has to be created for the rotor and the OGV each. These data sets comprise a parametric description of the blade and a table containing lift and drag coefficients for airfoil sections at different radial positions. For each radial section a representative airfoil geometry has to be extracted from the blade and the aerodynamic coefficients have to be determined for different angles of attack. It is recommended to provide lift and drag from $C_{L,min}$ to $C_{L,max}$ and to resolve the lift curve fine enough to capture the shape of the curve. With this data the blade forces are then computed using blade element theory. A detailed description of the technical implementation can be obtained from [10, 11] and further details on input data generation and performance can be found in [6].

C. RANS BodyForce

By modeling the engine with a body force model the engine blades are replaced by volume specific source terms reproducing the blade forces imposed to the flow. The forces are smeared out in tangential direction therefore there is no natural unsteadiness as usually observed for turbomachinery flow. No blade geometry is present in the computational mesh, nevertheless the model benefits from a refined mesh close to the axial position that would be swept by the blade's leading and trailing edges. The reason for this are strong gradients in the source terms at these positions which need sufficient discretization. An example mesh is depicted in Fig. 3 showing refinement at the blade leading and trailing edge positions. In addition the Chimera overlapping areas are visible in front of and behind the blades indicated by denser mesh lines. As for the actuator disk approach the usage of Chimera is not a prerequisite.

Body force modeling is available by a python interface and the Flowsimulator framework [12]. The TAU solver is thereby coupled with a body force module. Flow data and source terms are exchanged between the solver and the body force model. After obtaining an initial solution the flow state in the cells swept by the blades is communicated to the body force module. The body force model then computes source terms for the right hand side of the RANS equations representing engine performance. These source terms are then communicated back to the flow solver and added to the equations in the affected cells. The flow solver is then run for a user defined number of iterations until the body force module is called again. This loop is repeated until externally defined convergence criteria are met.

Before performing the first simulation the body force model is calibrated using performance data from the engine design process in the form of either 0D or 1D performance metrics. The computation of the source terms is done using Hall's model [13] with modifications introduced by Thollet[14]. A more detailed description of the body force method in use can be obtained from [14] and [15].

D. RANS Mixing Plane

With a RANS based approach using classical single passage simulations with mixing-planes between the stages an efficient performance assessment of the engine is possible for the entire engine operating range [2, 16]. Separate mesh

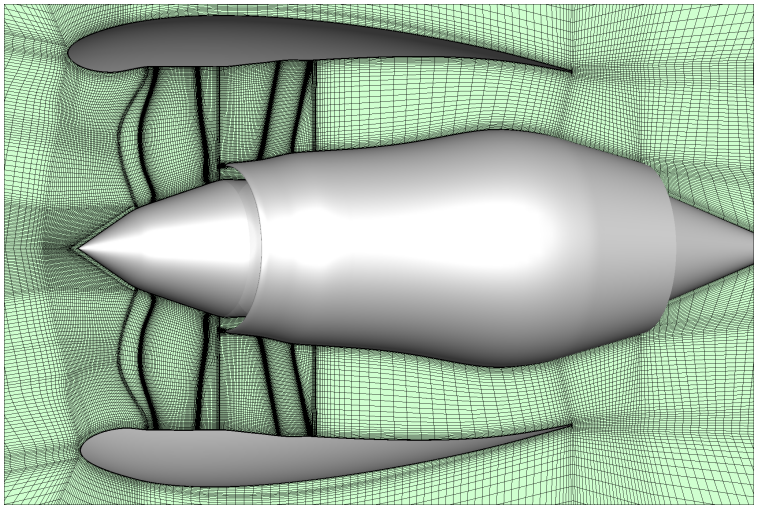

Fig. 3 Visualization of the mesh used for TAU RANS simulations with the body force model.

blocks around a rotor and a stator blade are created. By taking advantage of the mixing-plane approach through which the averaged steady state flow fields of rotor and OGV are coupled it is possible to model engine performance with a single passage simulation. Due to neglecting transient phenomena local time stepping can be used, typically resulting in a gain of computational efficiency by more than an order of magnitude compared with uRANS approaches, which makes this approach an efficient yet accurate approach used in a design context [17]. An example of a single passage setup as used during fan design can be seen in Fig. 4.

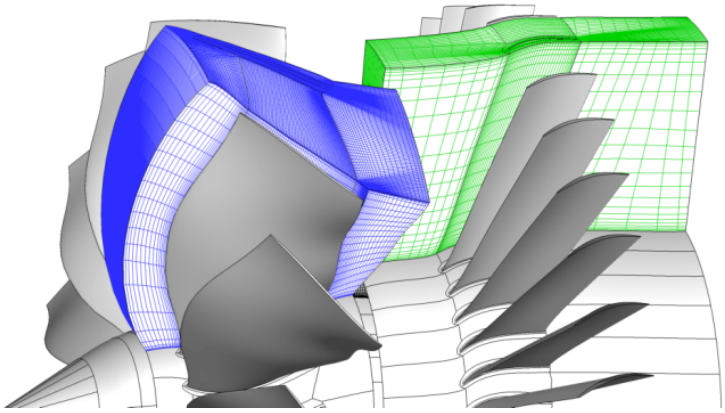

Fig. 4 Visualization of the mesh used for TRACE RANS mixing plane and uRANS simulations.

As a basis to study the transient fan and intake interaction, a RANS approach has also been used to couple the 360° meshed intake with single passage of the rotor, core section and OGV; results of this approach, here merely used to initialize the uRANS simulation, are shown in Fig. 10, yielding averaged performance parameters close to the time accurate simulations of the entire system; a similar observation has already been reported in [2].

E. uRANS Phase Lag

uRANS computations can be run on a single passage or on a full 360° annulus of the entire fan/intake system of selected blade rows thereof. Here results of the phase-shifted boundary conditions were applied allowing for an efficient means to study non-linear intake/rotor interactions by coupling the aforementioned 360° meshed intake with a single passage of the rotor and the OGV and hence accounting for typical angle-of-attack or crosswind scenarios [18]. A fully conservative zonal approach is used to interchange the flow data between the rotating rotor stage and the stationary

OGV stage. As an alternative, non-linear approach, the harmonic balance method was also applied in a post-design assessment effort (see e.g. [19]). This offers a further and in most cases substantial performance benefit compared with the previously mentioned single-passage and uRANS simulations due its formulation in the frequency domain whilst maintaining a high fidelity due to its non-linear nature.

V. Evaluation of Engine Modeling Methods

In the following the different engine modeling approaches are compared and evaluated for their capabilities. Not all modeling methods were available for all test points selected. A full annulus TRACE uRANS was not available for comparison. The engine operating points investigated are depicted in Table 1. Note that the simulations performed with the solver TRACE were performed for equivalent sea level static conditions while the TAU simulations used the actual flight conditions resulting in a deviation in Reynolds number by a factor of about 2. In a previous study it was shown that this does have a small impact on engine mass flow and stage total pressure ratio[3]. In addition the reduced Reynolds number under flight conditions results in a small decrease in efficiency compared to sea level static conditions due to the thicker boundary layers, increased aerodynamic friction and more pronounced secondary flow losses [3].

Table 1 Investigated engine operating points for the ASPIRE UHBR test case.

	Altitude [ft]	Mach Number [-]	Incidence Angle [°]
ADP: Aerodynamic Design Point	35000	0.8	3
SID: Take-Off Sideline	700	0.27	15

A. Aerodynamic Design Point

The aerodynamic design point as visible from Table 1 is a high speed operating condition used in cruise. TRACE mixing plane results from this operating point were used to calibrate the body force model and to define the boundary conditions to create the input data for the actuator disk model.

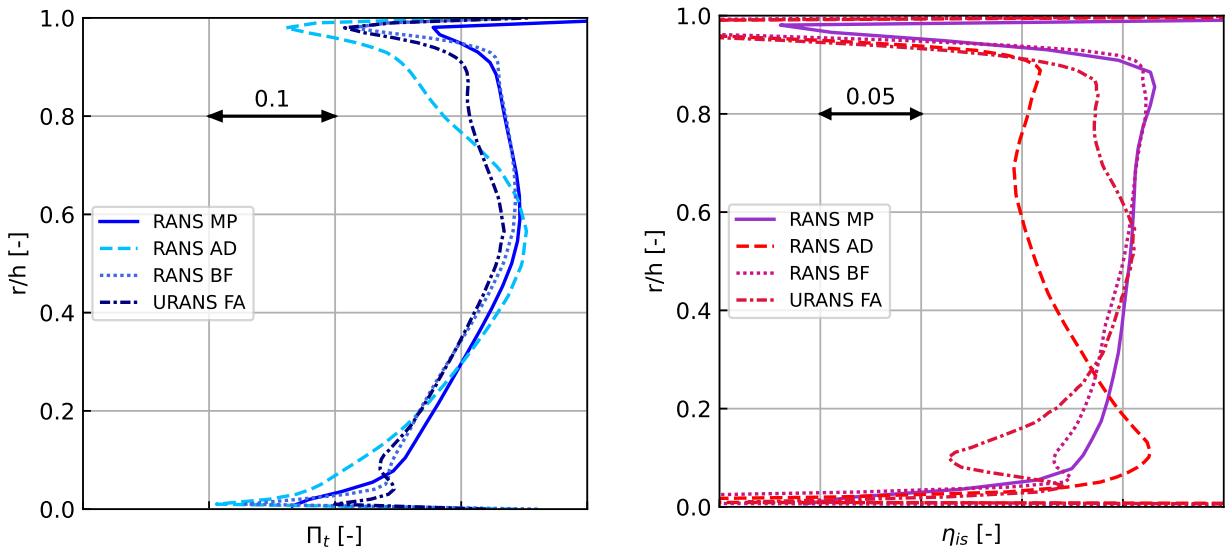

(a) Stage Total Pressure Ratio **(b) Stage Isentropic Efficiency**

Fig. 5 Radial distribution of stage performance metrics for ADP (mass weighted average)

Figure 5 shows radial distributions of fan performance for the different metrics investigated. The data is averaged in circumferential direction using density as a weighting function. The ordinate axis denotes non dimensional channel height. For the TRACE solver only RANS mixing plane results are shown since uRANS computations do not yield

any relevant additional information in terms of performance metrics for this design point.A radial distribution of the averaged stage total pressure ratio is depicted in Fig. 5a. The shape of the RANS mixing plane profile is very well matched by the body force model and the TAU uRANS curves, but the latter fails to reach the level of the mixing plane results and predicts the total pressure ratio to be slightly lower. The deviation of the TAU uRANS data and the mixing plane results is slightly larger in the upper half of the duct than in the lower half. The very good agreement of the body force method with the mixing plane data stems from the fact that the TRACE data of this operating point was used to calibrate the body force model. The actuator disk simulation is only able to reach the total pressure ratio of the mixing plane computation in a region at half duct height ($0.3 < r/h < 0.6$). In the hub and tip area the actuator disk model results in a significantly lower pressure ratio than all other methods presented with the deviations being much more pronounced at high radii.

A very sensitive performance metric in turbomachinery modeling is the stage isentropic efficiency shown in Fig. 5b. With the TAU uRANS approach it is possible to reproduce the mixing plane data at half duct height while significant losses can be observed in the hub and tip area with the hub losses being of a more severe nature. The efficiency of the uRANS simulation drops by around 5% at $r/h = 0.1$ before recovering again closer to the wall and then deteriorating once the wall boundary layer is reached. The reason for this behavior is a small flow separation occurring on the suction side of the OGV blades at this radius over the entire circumference. Comparing the efficiency results of the body force simulation with the TRACE data a very good agreement in shape and absolute levels can be observed. This is again owed to the fact that the body force model is used at its calibration point in this case. The TAU actuator disk model fails to predict the shape of the isentropic efficiency curve. In the hub region it shows a local maximum and strongly overestimates the efficiency. Towards higher radii a negative efficiency gradient can be observed that is not shown by any of the other methods investigated. In the tip region the actuator disk model efficiency increases again but stays significantly below what all other methods predict.

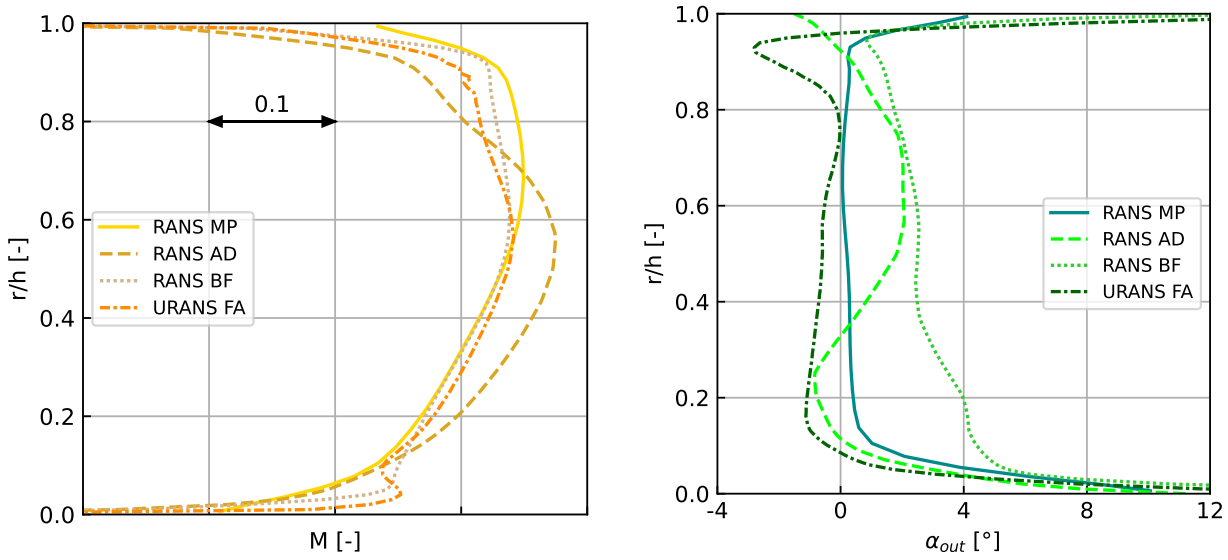

(a) OGV exit Mach number

(b) OGV outflow swirl angle

Fig. 6 Radial distribution of OGV exit conditions for ADP (mass weighted average)

The models were likewise tested for their ability to predict the fan stage exhaust profiles. In order to evaluate this, Mach number and swirl angle distributions where extracted just downstream of the OGV. Figure 6a shows the Mach number distribution for the three TAU modeling approaches and the mixing plane computation. Both the uRANS simulation and the body force approach are capable of reproducing the exhaust Mach number distribution of the mixing plane computation with high accuracy. Again the body force model fits the TRACE data even better than the uRANS simulation. The actuator disk model, although reaching comparable Mach number levels in the exhaust, predicts the profile to be more bulbous with stronger curvature compared to the other methods. It is evident that the shortcomings of the actuator disk model to predict the Mach number distribution is directly linked to its inability to accurately reproduce the stage total pressure ratio distribution.

The swirl angle just downstream of the OGV ist depicted in Fig. 6b with the orientation set such that negative angles correspond to the OGV stage overcorrecting the rotor swirl. For maximum efficiency the remaining swirl in the exhaust profile should be minimized which can be observed for the mixing plane simulation. For most of the duct height the outflow swirl angle is almost zero. Since these mixing plane simulations were being used to design this fan stage this comes as no surprise. The full annulus uRANS simulation is also able to reproduce this behavior for most of the channel height although the remaining swirl flow angle is slightly higher. At around 90% duct height a peak of the swirl angle in negative direction can be seen which is related to a corner vortex originating from the intersection of the OGV blade with the shroud. The actuator disk model shows larger deviations in swirl angle than the two previously discussed methods with the overall performance still being comparable. In the midspan region the actuator disk model delivers positive outflow swirl angles indicating that the redirection of the flow due to the OGV actuator disk is too strong in this area. In contrast to the previous analyses the body force model shows significantly larger deviations. The remaining absolute swirl in the exhaust flow is much larger than any other method predicts. This effect is most pronounced with small radii while the swirl angles in the tip region almost match what the other methods predict.

The comparison of integral engine performance metrics for the ADP case is shown in Fig. 7. A direct comparison between the data shown in Fig. 7 and the previously discussed radial distributions is inherently compromised for the mixing plane approach. It was not possible to apply the exact same turbulent boundary conditions for the far field setup with intake and the isolated fan stage setup because of the decay of turbulence over the large distance for the former setup, here leading to a decreased isentropic efficiency. This trend is however counteracted by the fact that the higher Reynolds number at sea level conditions increases isentropic efficiency, thus the relations between the different methods in terms of efficiency might appear different than what was observed in Fig. 5 and 6.

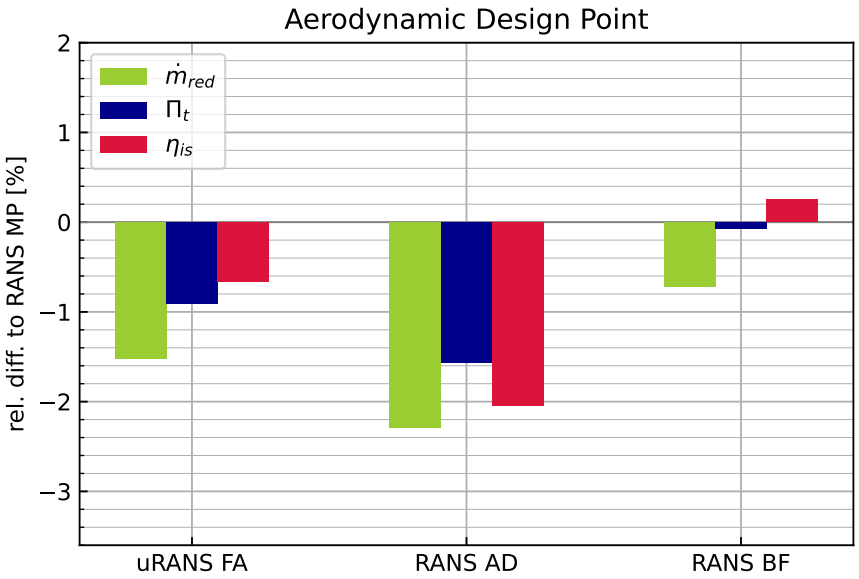

Fig. 7 Aerodynamic fan performance for all methods investigated (ADP)

The full annulus uRANS simulation predicts the fan mass flow 1.5% lower and the stage total pressure ratio about 1% lower than the mixing plane simulation. Stage isentropic efficiency nevertheless is computed within 0.7% of the mixing plane results giving confidence in the overall accuracy of the TAU uRANS method. The fact that the RANS mixing plane reference data was computed with a significantly higher Reynolds number at sea level conditions has to be taken into consideration and might explain these deviations.

The actuator disk model overall shows the largest deviations compared to the mixing plane simulation. Mass flow and isentropic efficiency are underestimated by just over 2% and stage total pressure ratio is computed to be 1.5% lower than the TRACE results. As already inferred in the discussion on radial distributions the agreement between the body

force simulation and the TRACE results is excellent. Largest deviations can be observed for the fan mass flow being 0.7% lower while isentropic efficiency and total pressure ratio match the data with high accuracy.

Overall the body force approach is best at reproducing the engine performance metrics at the aerodynamic design point. Mass flow, total pressure ratio and efficiency are predicted precisely compared to the TRACE results. A deficit observed for the model in this case was the remaining flow swirl aft of the OGV stage. The actuator disk model shows the largest deviations overall but still gives a useful estimate of engine performance. The full annulus uRANS simulation is able to accurately reproduce the radial distributions while slightly underestimating mass flow and total pressure ratio. The reader should be aware that the engine efficiency is very sensitive to small variations in the surrounding conditions and these results concerning engine efficiency should therefore be critically questioned. In summary the statement can be made that the overall spread of the results obtained from the different methods is comparable to levels observed in previous studies on the ASPIRE fan [3, 5, 20].

B. Take-Off Sideline

The sideline operating condition represents an acoustic certification point [3] but is hereby used to test the methodologies for a high power setting at low altitude. In addition the off-design performance of the actuator disk model and the body force model is tested this way as for both methods only data from the ADP condition was used to create their respective input data sets. Furthermore contrary to the discussion on ADP in chapter V.A the discrepancy in Reynolds number between the TAU and the TRACE simulations can be neglected since the flight altitude of the sideline case is fairly close to sea level conditions.

In Fig. 8a the circumferential mass weighted average of the stage total pressure ratio is depicted. As already observed for the ADP the TAU uRANS and body force simulation agree very well with the results from the mixing plane computation. The body force model results in a slightly higher total pressure ratio for large radii compared to the RANS mixing plan data while the full annulus uRANS results again slightly underestimate the total pressure ratio in the upper half of the duct. The actuator disk method fails to reach the overall levels of the TRACE simulation. Apart from a small region in the middle of the duct large deficits in stage total pressure ratio can be observed being most pronounced towards the shroud.

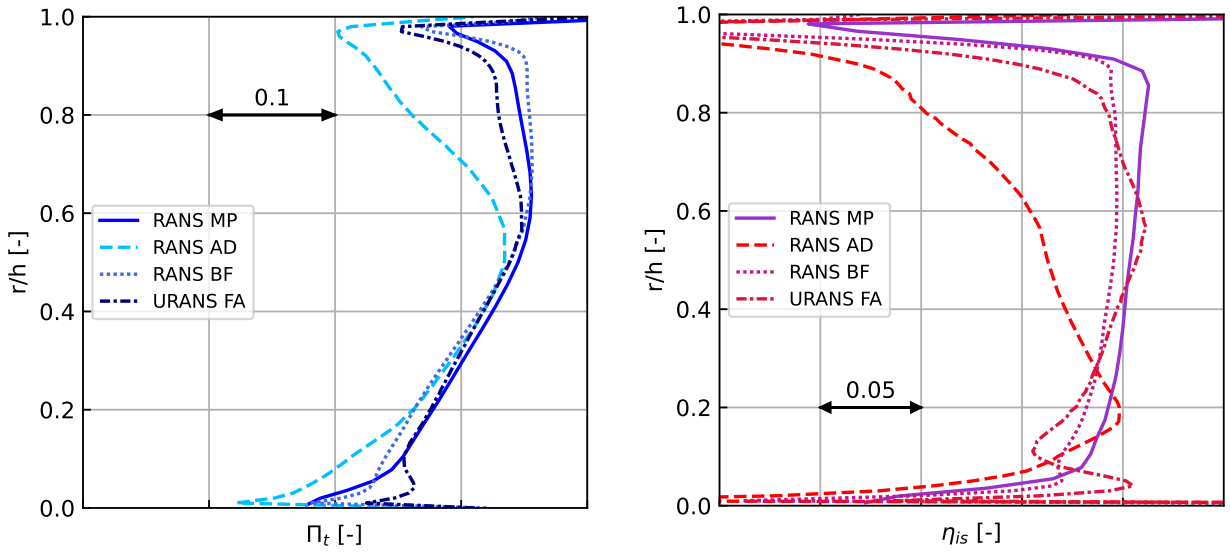

(a) Stage Total Pressure Ratio **(b) Stage Isentropic Efficiency**

Fig. 8 Radial distribution of stage performance metrics for SID (mass weighted average)

The distribution of isentropic efficiency in Fig. 8b shows a very good agreement between the full annulus uRANS and body force simulations and the RANS mixing plane data. As observed for the ADP the body force model fits the mixing plane data even better than the full annulus uRANS simulation does although a small offset is visible. The

uRANS simulation again suffers a drop in efficiency at around 10% duct height due to a flow separation occurring in the OGV stage. The actuator disk model shows a very different behavior in isentropic efficiency distribution than the other methods and is only able to reach the levels of the mixing plane simulation in the hub area. With increasing radius the efficiency continuously deteriorates showing deviations of up to 10% compared to the other methods in the tip region. It should be noted that the TAU RANS simulation using the actuator disk method exhibited a large flow separation over the entire circumference at the hub of the OGV disk extending over a significant length into the nozzle. It is assumed that this is related to the non-rotating OGV actuator disk interacting with the boundary layer flow, nevertheless further analysis is necessary to understand this behavior.

For this operating point the nozzle flow was evaluated as well. Figure 9a shows the average radial Mach number distribution just downstream of the OGV. The result of the RANS mixing plane simulation is best reproduced by the body force approach and the full annulus uRANS simulation both yielding a very similar radial distribution. While the agreement of the curves is very good in the lower half of the duct the deviation of the TAU simulations to the TRACE data increases in the upper half. All TAU methods predict a lower Mach number than the TRACE simulation towards the shroud. The actuator disk simulation again shows a much more bulbous Mach number distribution with the maximal Mach number occurring towards the middle of the duct instead of the upper half. Nevertheless the maximum Mach number is similar to the maximum Mach number observed for the mixing plane simulation.

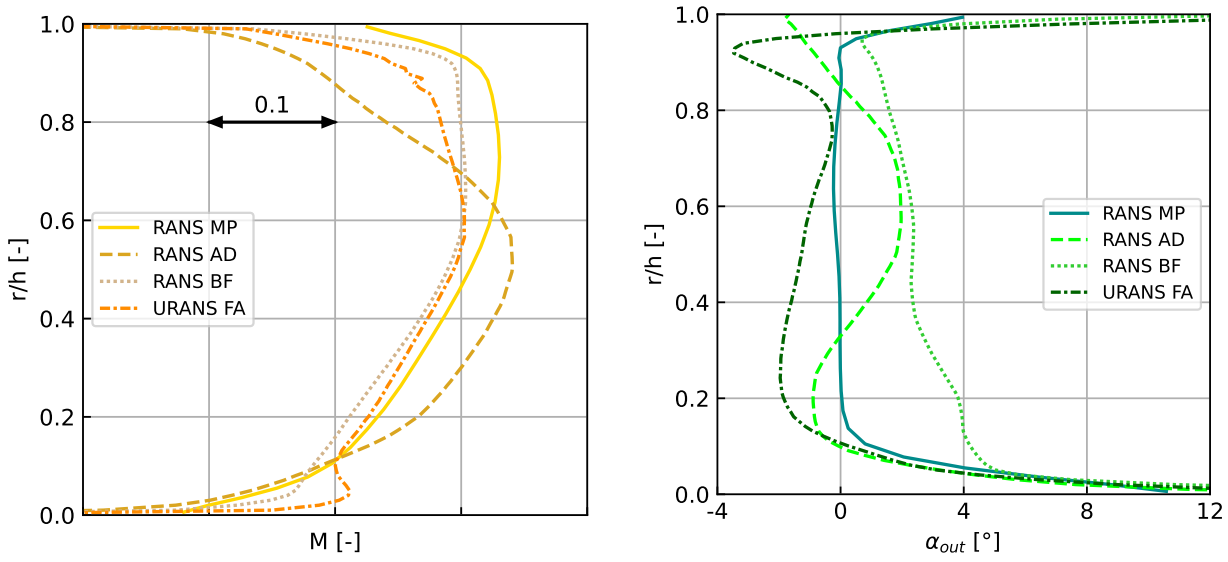

(a) OGV exit mach number **(b) OGV outflow swirl angle**

Fig. 9 Radial distribution of OGV outflow conditions or SID (mass weighted average)

As a final parameter the OGV outflow swirl angle is considered in Fig. 9b showing that the swirl is removed over almost the entire radius in the mixing plane simulation. The outflow swirl angles of the actuator disk and full annulus uRANS simulations are slightly larger than what was observed for the ADP case but still close to axial flow. With the TAU uRANS method the fan swirl is overcorrected in the OGV stage resulting in a slight swirl flow in the opposite direction of the fan rotation. The actuator disk model shows deviations of the swirl towards both directions depending on the local radius. The body force model, as observed for the ADP shows the largest outflow swirl angles of all methods with a significant amount of swirl flow in the direction of fan rotation remaining downstream of the OGV.

In the following the integral performance results for the SID case are discussed. For this operating point results of a TRACE uRANS simulation with phase-shifted boundary conditions were available for comparison as well. The results for all methods are shown in Fig. 10. Again, as for the ADP case, the reader should be aware that the TRACE simulation used as reference point was performed with different inlet conditions resulting in a change in inflow turbulence intensity which in turn has a negative impact on engine isentropic efficiency. In addition no significant Reynolds number effect counteracting this trend is present for the sideline case. Following these remarks the relations between the different

methods in terms of efficiency might appear different than what was observed in Fig. 8 and 9.

The difference between the TRACE uRANS simulation and the TRACE RANS single passage mixing plane approach are negligibly small supporting the statement made for the ADP that a TRACE uRANS simulation does not yield any additional information on overall performance compared to a single passage mixing plane simulation close to the engine design point. The TAU uRANS simulation is also capable to reproduce the mass flow and stage total pressure ratio with very high accuracy while the isentropic efficiency is overestimated by over 1.2% with this approach. The body force model predicts the mass flow to be around 1% lower while the stage total pressure ratio of the mixing plane data is accurately matched. Deviations in efficiency are comparable to results obtained with the full annulus uRANS approach. Nevertheless, although being applied outside its calibration point, the results of the body force model are still of acceptable accuracy. The actuator disk simulation instead shows much larger deviations for all three parameters with of about 3%. The reason for these larger performance deviations may be linked to the observed flow separation at the hub of the OGV actuator disk mentioned earlier.

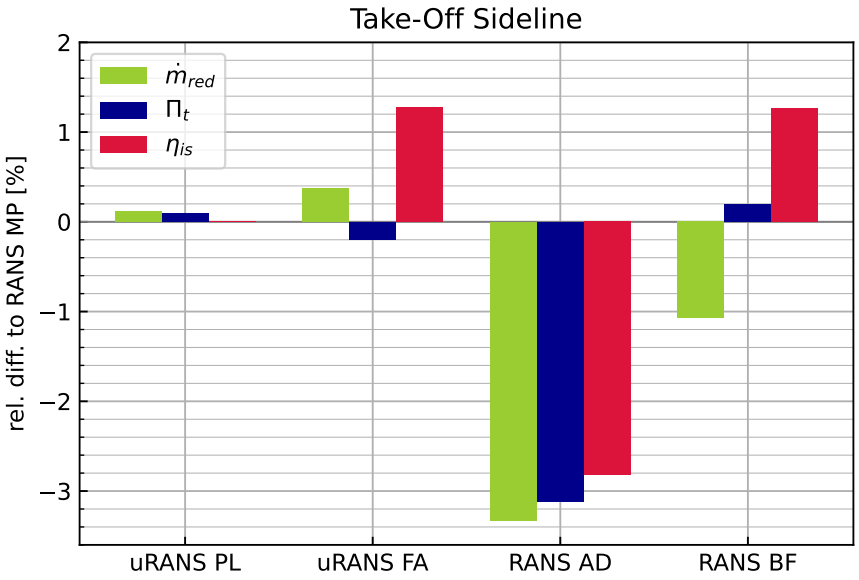

Fig. 10 Aerodynamic fan performance for all methods investigated (SID)

VI. Discussion

In the following a discussion on the various advantages and disadvantages of the methods from a user perspective is given. The previously presented findings are assessed and put into context.

A. uRANS Full Annulus

Unsteady computations with rotating fan blades are the most accurate but also the most expensive and time consuming approaches in TAU. This results from the fact that a TAU uRANS simulation of an engine always has to account for the entire circumference due to the lack of suitable boundary interfaces between rotor and stator applicable in single passage flow. With the uRANS method it is possible to capture detailed unsteady blade interactions of rotor and stator and aeroacoustic effects [9]. Thus the convection of the rotor wake areas to the stator is well captured. Additionally non-periodic circumferential 3D blade to blade effects are considered.

As shown in chapter V it is possible to reproduce integral engine performance with high accuracy for different operating conditions. In addition the uRANS approach can reproduce a representative radial distribution of the engine flow for various key performance parameters. Its capabilities to account for non-uniform inflow as presented in [9] prove that this method is well suited to investigate engine integration effects. Thus, within the uRANS simulation the

inhomogeneous engine inlet conditions are captured for a defined number of circumferential rotated rotor positions. This allows the high-fidelity simulation of unsteady internal flow phenomena for any inflow condition (e.g. crosswind, farfield).

Nevertheless due to its vast demands for computational resources and the complexity of meshing an entire fan stage it is not suitable for any design work. Even with access to modern HPC systems it takes at least weeks to perform this kind of simulation. In addition the mesh requirements in terms of resolution and alignment of the cells at the Chimera boundaries make the mesh generation a very intricate task. The area of application of the TAU uRANS approach lies in post-design evaluation studies on isolated nacelles and integrated engine-airframe configurations and to provide validation or calibration data for high-fidelity engine models like the actuator disk approach or the body force method.

B. RANS Actuator Disk

The actuator disk method in TAU is able to capture mean aerodynamic quantities of fan engine flow with fair accuracy as discussed in chapter V. The ability to accurately reproduce radial distributions is limited but it is possible to obtain a fair representation of post OGV nozzle flow with the actuator disk model. Its direct integration into the TAU code makes it an efficient tool to reproduce averaged fan engine flow quantities for different operating points and different external flow conditions. The computational overhead compared to a RANS simulation with classical one-dimensional boundary conditions is only moderate and amounts to approximately 10%. Mesh generation for an actuator disk setup in TAU is possible with many commercially available meshing tools. The actuator disk method does not have any special requirements for the grid resolution that deviate from those of any other RANS simulation. The actuator disk is modeled as a disk of zero thickness and can therefore not account for effects due to the metal blockage of the blades which distinguishes it from all other methods presented.

The actuator disk in TAU relies on information of sectional lift- and drag-coefficients provided for different radial positions and therefore requires knowledge of the blade geometry. Depending on airfoil properties and number of radial sections the 2D simulations performed to obtain lift and drag coefficients can require a significant amount of computation time. In addition precise data of the local flow conditions close to the blades is required and has to be incorporated into the 2D simulations. This information can for example be obtained from simulations run during the engine design process which usually incorporates a through-flow method or (u)RANS simulations. This way the method can be used during aircraft/engine design and integration.

Nevertheless once the input data set is created for one engine operating point the actuator disk can be used to model engine performance under different flow conditions and operating points giving results within a day on a modern HPC cluster thus justifying the effort for input data generation. The accuracy of the results may deteriorate with increasing distance to the original operating point the input data was created for as discussed in chapter V.B. At this time it is not possible to incorporate calibration for different operating points in one data set but it is possible to create a distinct data set for each operating point if required to improve performance at a specific flow condition. Careful data selection and process automation may help to reduce the effort to create the input data set.

C. RANS Body Force

Using the body force model with the DLR TAU Code allows to perform accurate simulations of mean turbomachinery aerodynamics for different flow conditions and operating points. This holds true for both integral engine performance and radial distributions as shown in Fig. 5 - 10. The computational overhead is slightly larger compared to the actuator disk method but of a similar magnitude. The body force model can be calibrated for different engine operating conditions and is able to incorporate metal blockage effects although no actual blade is incorporated in the mesh. The calibration can be done with different levels of fidelity with increasing complexity for more advanced calibration methods. The calibration effort, although of a completely different nature, is comparable to the actuator disk model. Precise knowledge of the engine and blade geometry as well as engine performance metrics is required in order to apply the model.

A disadvantage of the model is its violation of mass continuity when accounting for metal blockage. The blockage source terms modify the continuity equation which may result in significant changes to the engine massflow when the spatial resolution of the body force region is insufficient. It is therefore recommended to increase the grid density in the mesh regions where the blade leading and trailing edges would sweep the mesh (see Fig. 3) to minimize this effect. Due to its direct integration to the FlowSimulator environment the model can be flexibly integrated to more advanced CFD setups and optimizations. Once calibrated the relatively fast turnaround time of computations with the body force model and its capability to model different engine operating points make it well suited for aircraft-engine integration studies.

D. RANS Mixing Plane

With the mixing plane approach the main flow features and performance characteristics of the engine can be quantified with very moderate requirements in terms of computation time. The latter is due to the fact of smaller meshes compared to the other shown RANS approaches. The presence of circumferential periodicity of rotor/stator blades allows to reduce a full annulus mesh to a single passage setup mesh by placing the mixing plane between the rotor/stator interface. The approach provides a good compromise in terms of accuracy and numerical cost for turbomachinery aerodynamics. Thus it is an efficient approach for the blade annulus 3D design process. As seen in Fig. 7 the performance characteristics are showing a good agreement for small inhomogeneities in inlet conditions.

Nevertheless with the single passage mixing plane approach it is not possible to capture unsteady or increased circumferential inhomogeneous (e.g. crosswind, climb, descend) rotor/stator engine inlet boundary conditions physically adequately. This results from averaging the flow field between the two blades, which mixes out inhomogeneities in circumferential direction at the interface (e.g. wake areas). Hence, it is not possible to capture aeroacoustic blade interaction. At least for a single passage it is however possible to consider farfield or crosswind conditions and evaluate the impact on the passage.

E. uRANS Phase Lag

Single passage uRANS simulations with time shifted boundary conditions allow it to resolve unsteady effects within a single passage without having to mesh and compute a full annulus engine setup. This way unsteady internal flow phenomena and the interaction of the fan stage with different homogeneous inflow conditions can be simulated with high fidelity. Thus rotor and stator interactions can be adequately quantified. For the simulation setup the same meshes as for RANS single passage can be used by replacing the mixing plane with a zonal interface. Due to the fact that only one passage is represented this method cannot account for a variation in boundary condition at different circumferential positions within one simulation and no direct coupling to the flow of the surrounding geometry (e.g. aircraft, nacelle) can be assessed. Nevertheless, it is possible to consider crosswind and farfield effects for one passage or a rough overview over the whole engine is given by circumferential averaging inlet boundary conditions. This approach delivers averaged performance results close to the RANS mixing plane approach (compare Fig. 10) but with higher fidelity in terms of analyzing 3D effects.

VII. Conclusion and Outlook

In this paper we gave an overview over a variety of aerodynamic engine modeling methods with the flow solvers TAU and TRACE. For RANS simulations a single passage mixing plane approach, an actuator disk model and a body force model were investigated. To allow for the ability to resolve unsteady effects within uRANS simulations a full annulus setup incorporating the entire engine circumference and a single passage setup using phase-shifted boundary conditions were considered. Accurate results can be obtained by performing full annulus uRANS computations but even with state of the art HPC systems these approaches are only suitable for post-design evaluation due to their long turnaround time and high cost. A compromise in terms of fidelity and cost when it comes to unsteady effects is given by single passage uRANS simulations with phase shifted boundary conditions still capturing unsteady aerodynamics while only having to model one blade passage. The body force model and the mixing plane approach allow to estimate mean engine performance within RANS simulations with fast turnaround times and high accuracy within RANS simulations. The actuator disk method is less accurate in terms of radial profiles and integral performance metrics but still delivers useful results. Nevertheless the actuator disk and body force simulations rely on reference flow data close to the blades for calibration. In addition all methods require knowledge of the actual blade geometry to accurately reproduce engine performance. The effort to prepare the input data for the actuator disk and body force models is not negligible but once a calibrated input data set is available the methods deliver fast results for different operating conditions. An embedding of the actuator disk and body force models into more complex aircraft-engine configurations is possible allowing to assess installed engine performance making them suitable for an integrated engine airframe design approach.

Future work may address the behaviour of the actuator disk model under off design conditions and the ability to incorporate calibration data from different operating points. A thorough understanding of the hub separation with the actuator disk in off design has to be obtained to counteract this behaviour. In addition an improvement of the calibration processes for the actuator disk and body force models could be introduced to reduce the workload for the user and improve off design performance. After now having assessed these methods for an isolated configuration their capabilities to reproduce installed performance for a distorted inflow case (e.g. BLI) will be assessed in future studies.

References

[1] Gerhold, T., "Overview of the Hybrid RANS Code TAU," *MEGAFLOW - Numerical Flow Simulation for Aircraft Design*, edited by N. Kroll and J. K. Fassbender, Springer Berlin Heidelberg, Berlin, Heidelberg, 2005, pp. 81–92.

[2] Becker, K., Heitkamp, K., and Kuegeler, E., "Recent Progress in a Hybrid-Grid CFD Solver for Turbomachinery Flows," *V European Conference on Computational Fluid Dynamics ECCOMAS CFD*, 2010.

[3] Schnell, R., Golfhahn, E., and Julian, M., "Design and Performance of a Low Fan-Pressure-Ratio Propulsion System," *25th International Symposium on Air Breathing Engines ISABE 2019*, Canberra, Australia, 2019.

[4] Meheut, M., Sartor, F., Vergez, M., Laban, M., Schnell, R., Stuermer, A. W., and Lefevre, G., "Assessment of Fan/Airframe aerodynamic performance using 360° uRANS computations: Code-to-Code comparison between ONERA, DLR, NLR and Airbus." *AIAA SciTech Forum, 7-11 January 2019, San Diego, California*, American Institute of Aeronautics and Astronautics, 2019. https://doi.org/10.2514/6.2019-0582.

[5] Burlot, A., Sartor, F., Vergez, M., Méheut, M., and Barrier, R., "Method Comparison for Fan Performance in Short Intake Nacelle," *2018 Applied Aerodynamics Conference*, American Institute of Aeronautics and Astronautics, 2018. https://doi.org/10.2514/6.2018-4204.

[6] Spinner, S., Keller, D., Schnell, R., and Trost, M., "A Blade Element Theory Based Actuator Disk Methodology for Modeling of Fan Engines in RANS Simulations," *AIAA Aviation 2020*, 2020. https://doi.org/10.2514/6.2020-2749.

[7] Madrane, A., Heinrich, R., and Gerhold, T., "Implementation of the Chimera Method in the Unstructured Hybrid DLR Finitve Volume TAU-Code," *6th Overset Composite Grid and Solution Technology Symposium*, Ft. Walton Beach, FL, USA, 2002, pp. 524–534.

[8] Spalart, P., and Allmaras, S., "A one-equation turbulence model for aerodynamic flows," *30th Aerospace Sciences Meeting and Exhibit*, 1992.

[9] Stuermer, A., "DLR TAU-Code uRANS Turbofan Modeling for Aircraft Aerodynamics Investigations," *Aerospace*, Vol. 6, No. 11, 2019, p. 121. https://doi.org/10.3390/aerospace6110121.

[10] Raichle, A., Melber-Wilkending, S., and Himisch, J., "A New Actuator Disk Model for the TAU Code and Application to a Sailplaine with a Folding Engine," *New Results in Numerical and Experimental Fluid Mechanics VI*, edited by C. Tropea, S. Jakirlic, H.-J. Heinemann, R. Henke, and H. Hönlinger, Springer Berlin Heidelberg, Berlin, Heidelberg, 2008, pp. 52–61.

[11] Raichle, A., "Flux Conservative Discretization of the Actuator Disk Model as a Discontinuity Surface," Ph.D. thesis, Technical University Braunschweig, 2017.

[12] Meinel, M., and Einarsson, G. O., "The FlowSimulator framework for massively parallel CFD applications," *PARA 2010*, Reykjavik, Island, 2010.

[13] Hall, D. K., "Analysis of Civil Aircraft Propulsors with Boundary Layer Ingestion," Ph.D. thesis, Massachusetts Institute of Technology, 2015.

[14] Thollet, W., "Body force modeling of fan-airframe interactions," Ph.D. thesis, University of Toulouse, 2017.

[15] Thollet, W., Dufour, G., Carbonneau, X., and Blanc, F., "Body-force modeling for aerodynamic analysis of air intake – fan interactions," *International Journal of Numerical Methods for Heat & Fluid Flow*, Vol. 26, No. 7, 2016, pp. 2048–2065. https://doi.org/10.1108/hff-07-2015-0274.

[16] Franke, M., Röber, T., Kügeler, E., and Ashcroft, G., "Turbulence treatment in steady and unsteady turbomachinery flows," *Fifth European Conference on Computational Fluid Dynamics ECCOMAS CFD*, Lisbon, Portugal, 2010.

[17] Schnell, R., and Corroyer, J., "Coupled Fan and Intake Design Optimization for Installed UHBR-Engines with Ultra-Short Nacelles," *23rd International Symposium on Air Breathing Engines ISABE*, 2015.

[18] Schnell, R., "Investigation of the Acoustic Nearfield of a Transsonic-Fanstage by Time-Domain CFD-Calculations with Arbitrary Blade Counts," *ASME Turbo-Expo*, 2004.

[19] Frey, C., Ashcroft, G., Kersken, H., Schönweitz, D., and Mennicken, M., "Simulation of Indexing and Clocking with Harmonic Balance," *International Journal of Turbomachinery, Propulsion and Power*, Vol. 3, No. 1, 2017.

[20] Meheut, M., Sartor, F., Vergez, M., Laban, M., and Schnell, A., R. amd Stürmer, "Assessment of Fan/Airframe aerodynamic performance using 360° uRANS computations: Code-to-Code comparison between ONERA, DLR and NLR," *AIAA SciTech Forum*, 2019.